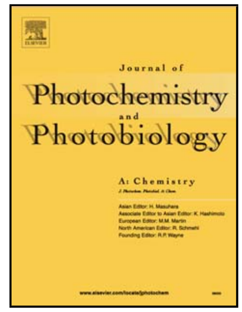


Title: Vacuum-UV photolysis of aqueous solutions of citric and gallic acids

Authors: Natalia Quici, Marta I. Litter, André M. Braun, Esther Oliveros

PII: S1010-6030(08)00025-7
DOI: doi:10.1016/j.jphotochem.2008.01.008
Reference: JPC 7988

To appear in: *Journal of Photochemistry and Photobiology A: Chemistry*

Received date: 26-11-2007
Revised date: 14-1-2008
Accepted date: 18-1-2008

Please cite this article as: N. Quici, M.I. Litter, A.M. Braun, E. Oliveros, Vacuum-UV photolysis of aqueous solutions of citric and gallic acids, *Journal of Photochemistry and Photobiology A: Chemistry* (2007), doi:10.1016/j.jphotochem.2008.01.008

# Vacuum-UV photolysis of aqueous solutions of citric and gallic acids

**Natalia Quici[a], Marta I. Litter[a], André M. Braun[b], Esther Oliveros*[b,1]**

[a]*Gerencia Química, Comisión Nacional de Energía Atómica, Av. Gral. Paz 1499, (1650) San Martín, Prov. de Buenos Aires, Argentina*

[b]*Lehrstuhl für Umweltmesstechnik, Universität Karlsruhe, 76128 Karlsruhe, Germany*

*quici@cnea.gov.ar*

*litter@cnea.gov.ar*

*oliveros@chimie.ups-tlse.fr*

*Andre.Braun@ciw.uni-karlsruhe.de*



* Corresponding author: Esther Oliveros, oliveros@chimie.ups-tlse.fr

[1] New permanent address: Laboratoire des IMRCP, UMR CNRS 5623, Université Paul Sabatier, 118, route de Narbonne, F-31062 Toulouse Cédex 9, France ; *Fax: +33-5-61558155; Tel: +33-5-61556968.*

**Abstract**

The vacuum-UV- (VUV-) photolysis of water is one of the Advanced Oxidation Processes (AOP) based on the production of hydroxyl radicals ($HO^•$) that can be applied to the degradation of organic pollutants in aqueous systems. The kinetics of the VUV-photolyses of aqueous solutions of citric acid (**1**) or gallic acid (**2**) were investigated in the presence or absence of dissolved molecular oxygen ($O_2$) and under different pH conditions. In the case of **1**, the rate of consumption of the substrate was faster at pH 3.4 than in alkaline solution (pH 11), whereas, in the case of **2**, the variation of pH (2.5 to 7.5) did not affect the course of the reaction. Unexpectedly, the rates of depletion of both **1** and **2** decreased in the absence of $O_2$, this effect being much more pronounced in the case of **2**. In order to explain these results, possible reaction pathways for the degradation of **1** and **2** are proposed, and the roles of the oxidizing ($HO^•$) and reducing ($H^•$ and $e^-_{aq}$) species produced by the VUV-photolysis of water are discussed.

Keywords: VUV-photolysis; advanced oxidation processes (AOP); water treatment; citric acid; gallic acid.

## 1. Introduction

Interested in exploring viable alternatives for water treatment, we have investigated the oxidation and mineralization of two model compounds, citric and gallic acids, using different Advanced Oxidation Processes (AOP). Citric acid (2-hydroxy-propane-1,2,3-tricarboxylic acid, **1**) is present in most of the fruit juices and is of general use as preservative in a variety of products of the food industry. In addition, the compound is used in cleaning and decontamination mixtures for boilers and cooling circuits of nuclear power plants. Gallic acid (3,4,5-trihydroxybenzoic acid, **2**) may be considered as one of the simplest models for natural organic matter, *i.e.* of humic and fulvic acids. The maximum contaminant level for gallic acid established by environmental protection organizations of Canada, USA and EEC is 2 mg $L^{-1}$ [1]. Gallic acid is one of the main constituents of herbal roots and tea leaves [2-3], and is present in wastewaters originating from olive oil factories and also from boiling cork [4]. Gallic and/or citric acids were proposed to be used in formulations in combination with EDTA or NTA for dissolving magnetite or hematite for the cleaning and decontamination of cooling circuits of nuclear reactors [5-6]. Gallic acid is considered to be a good antioxidant [3].

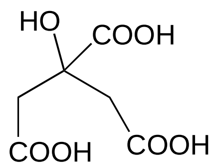


**1**

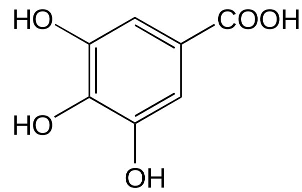


**2**

AOP are abiotic methods applied to the treatment of effluents in gaseous and condensed phases that involve the generation of very active oxidizing species [7]. For the purpose of oxidation and/or mineralization of organic matter in aqueous media, the hydroxyl radical ($HO^{\bullet}$) is the main and most reactive species generated [8-11], and is able to attack a large variety of organic compounds.

There are only a few published examples where the oxidative degradation of citric acid by AOP was investigated: $TiO_2$ photocatalysis was used to oxidize this organic substrate [12], in several cases in combination with the reductive removal of heavy metals [13-18]. Results of the oxidative degradation of citric acid by $TiO_2$ photocatalysis, the photochemically enhanced Fenton (photo-Fenton) process and a combination of the two methods were recently published [19].

A few articles deal with gallic acid degradation by AOP. The compound was chosen for investigations using UV photolysis, the combination $UV/H_2O_2$, the Fenton and photo-Fenton processes [4, 20, 21], the combination of biological treatment with a modified Fenton process [22], pyrylium salt photocatalysis [23] and ozonation [1, 24].

Investigations on the degradation of gallic acid by $TiO_2$ photocatalysis are currently in progress (Quici and Litter, to be published).

One of the most powerful AOP for the degradation of organic compounds is their VUV-photolysis in the gas phase [25-27] or the VUV-photolysis of their aqueous solutions [7, 8, 27,28]. Due to the high absorption cross-section of water, VUV-radiation, emitted by a $Xe_2$-excimer radiation source ($\lambda_{em}$: 172 ± 14 nm), is almost exclusively absorbed by $H_2O$, leading primarily to the homolysis of the O-H bond (equation (1)) [28].

$$H_2O + h\nu \rightarrow HO^{\bullet} + H^{\bullet} \quad (1)$$

The quantum yield of reaction (1) in liquid water depends on the wavelength of irradiation (0.42 at 172 nm) [29]. $HO^{\bullet}$ radicals react primarily by hydrogen abstraction (generally from aliphatic carbon atoms) or by electrophilic addition to $\pi$-systems [7]. With standard redox potentials of 2.7 V in acidic and of 1.8 V in neutral solution [30], $HO^{\bullet}$ may also oxidize organic compounds by electron transfer reactions.

Beside homolysis, VUV-irradiation (172 nm) of $H_2O$ also produces solvated electrons with a quantum yield of 0.05 (equation (2)) [27], the $e^-_{aq}$ being converted to $H^{\bullet}$ by $H_3O^+$ (reaction (3)) [30]:

$$H_2O + h\nu \rightarrow HO^{\bullet} + H^+ + e^-_{aq} \quad (2)$$

$e^{-}_{aq} + H_3O^+ \rightarrow H^{\bullet} + H_2O$ (3)

Hydrogen atoms may be involved in the reduction of organic substrates, but are quantitatively trapped by molecular oxygen ($O_2$) in aerated solutions (reaction (4)). $O_2$ may also be reduced by $e^-_{aq}$ (reaction leading to the formation of the superoxide anion ($O_2^{\bullet-}$, reaction (5)). The disproportionation of $O_2^{\bullet-}$ and its conjugated acid $HO_2^{\bullet}$ (reaction (6)) yields hydrogen peroxide (reaction (7)) [31]. Production of $H_2O_2$ during VUV-photolysis of water has been demonstrated [32].

$O_2 + H^{\bullet} \rightarrow HO_2^{\bullet}$ $k_4 = 2.1 \times 10^{10}\ M^{-1}\ s^{-1}$ [28] (4)

$O_2 + e^{-}_{aq} \rightarrow O_2^{\bullet-}$ $k_5 = 1.9 \times 10^{10}\ M^{-1}\ s^{-1}$ [28] (5)

$O_2^{\bullet-} + H_2O \leftrightarrows HO_2^{\bullet} + HO^-$ $pK_a = 4.8$ [33](6)

$O_2^{\bullet-} + HO_2^{\bullet} + H_3O^+ \rightarrow O_2 + H_2O_2 + H_2O$ (7)

In strongly alkaline solutions, $O^{\bullet-}$ is generated by the deprotonation of $HO^{\bullet}$ (reaction (8)). $O^{\bullet-}$ reacts more slowly than $HO^{\bullet}$ in electron transfer reactions and attacks preferentially $C(sp^3)$-centers of aryl compounds by hydrogen abstraction, while $HO^{\bullet}$ adds preferentially to the aromatic system [30].

$HO^{\bullet} + HO^- \leftrightarrows O^{\bullet-} + H_2O$ $pK_a = 11.9$ [30] (8)

The VUV-photolysis of water or aqueous systems may be used for ultrapure water production and for the degradation of pollutants dissolved in water and known to be mineralized only in reaction systems combining reductive and oxidative steps, such as perchlorinated hydrocarbons [34] or atrazine [35]. Parallel reduction and oxidation cycles were also found in VUV-photolyses of aqueous solutions of nitrate and nitrite, of ferri- and ferrocyanate as well as of model pollutants in the presence of nitrate and nitrite [36-39].

The high absorption cross-section of water and the present state of technology for generating high potentials at high frequencies prevent the development of the VUV-photolysis to the level of large scale units. However, the high quantum efficiency of $HO^{\bullet}$ generation without addition of any oxidant other than $O_2$ favors this process for production and treatment units of limited photonic fluxes.

In this work, results of the VUV-photolysis of aqueous solutions of **1** and **2** are reported and the effects of the concentration of dissolved $O_2$ and of the initial pH of the solutions discussed.

## Experimental

### *Chemicals*

Citric acid ($C_6H_8O_7.H_2O$, **1**, Fluka, 99,5%), gallic acid ($C_7H_6O_5.H_2O$, **2**, Riedel-De Haën, 99%) and 3-oxoglutaric acid (acetonedicarboxylic acid, propanone-1,3-dicarboxylic acid, $C_5H_6O_5$, **3**, Aldrich, technical grade) were used as supplied. Pure water was provided by a PURELAB PLUS system (USA). $NaH_2PO_4$ and phosphoric acid (Merck) were used for the preparation of the HPLC eluent.

*Photochemical reactor and excimer radiation source*

Irradiations were carried out in a loop-type photochemical reactor already described [29]. The reactor (400 mL) was equipped with a cylindrical $Xe_2$-excimer radiation source emitting at 172 (± 14 nm) and positioned in the central axis of the photoreactor. The radiation source consisted of two concentric Suprasil® quartz tubes (length: 25 cm, outer diameter: 3.0 cm) with an inner electrode (phase) made of an aluminum foil, cooled with distilled water. An additional Suprasil® tube was positioned between the outer wall of the light source and the reaction solution, providing a gap for the outer electrode. This outer electrode was made of an extensible net of stainless steel (wire diameter: 0.1 mm) and was connected to the ground. The gap between the two Suprasil® tubes was purged with $N_2$ to avoid filter effects by $O_2$. The $Xe_2$-excimer radiation source was driven by a high voltage power supply (ENI Model HPG-2) with an electrical power of 110W at 185-190 KHz. The radiant efficiency of the radiation source was approximately 8%. The reactor was immersed into a water bath kept at 20ºC.

*Irradiation experiments*

Experiments were performed with 370 mL of aqueous solutions of 0.5 to 2.0 mM of compounds **1** or **2**, and the initial pH was adjusted with 0.1 M HCl or 0.5 M

NaOH solutions. The solutions were introduced into the reactor and purged with synthetic air (30 min) or with $N_2$ (2 h) before irradiation. Continuous purging and magnetic stirring ensured good mixing of the solutions during the entire period of irradiation. Samples (1 mL) were taken periodically for analysis.

*Analytical techniques*

The evolution of the concentrations of **1** and **2** with irradiation time was followed by HPLC analysis [19]. The Hewlett-Packard liquid chromatograph model 1100 with diode array detector (detection wavelength for **1**: 210 nm, for **2**: 271 nm) was equipped with a LiChrosphere 100 RP C18 column (5 µm, 250 × 4 mm). The eluent consisted of 97% of 25 mM $KH_2PO_4$ at pH 2.3 ($H_3PO_4$) and 3% acetonitrile for **1**, and of 97% of 5 mM $KH_2PO_4$ at pH 2.3 ($H_3PO_4$) and 3% acetonitrile for **2** (flow rate: 1 mL $min^{-1}$; temperature: 20°C). 3-Oxoglutaric acid (**3**) was identified by co-injection. Total organic carbon (TOC) was measured with a Shimadzu 5000-A TOC analyzer in the NPOC (non-purgeable organic carbon) mode.

Experimental errors have been estimated to be 4% for the quantitative analysis of citric acid and 3% for that of gallic acid.

## 3. Results and discussion

### *3.1. Citric acid*

Preliminary VUV-photolyses were performed at three initial concentrations (0.5, 1.0 and 2.0 mM), at acidic pH (3.4) and under air bubbling. Profiles of the normalized concentration of **1** ([**1**]/[**1**]$_0$) *vs.* time of VUV-photolysis are shown in Figure 1. The rate of consumption of **1** increased with decreasing initial concentration ([**1**]$_0$). The pH of the reaction varied less than one unit during irradiation. TOC was found to decrease to 50% and 40% of $TOC_0$ after 180 min of irradiation time, in the cases of [**1**]$_0$ = 1.0 and 2.0 mM, respectively.

**Figure 1.** Consumption of citric acid (**1**) in air-equilibrated aqueous solution upon VUV-photolysis. Profiles of [**1**]/[**1**]$_0$ *vs.* time of irradiation at different initial concentrations of **1** ([**1**]$_0$); pH 3.4, 20°C.

The effects of the presence or absence of $O_2$ and of pH variation were investigated with solutions of [**1**]$_0$ = 0.5 mM, where the highest rate of depletion was found. The corresponding profiles of ln([**1**]/[**1**]$_0$) *vs.* time of irradiation are shown in Figure 2. Within experimental error, the depletion of **1** followed in all cases apparent first-order kinetics, and the corresponding rate constants ($k_{app}$) are listed in Table 1.

**Figure 2.** Depletion of **1** in aqueous solution upon VUV-photolysis. Profiles of ln([**1**]/[**1**]$_0$) *vs.* time of irradiation, for [**1**]$_0$ = 0.5 mM in presence or absence of $O_2$ and at pH 3.4 and 11.0.

**Table 1.** Apparent first-order rate constants ($k_{app}$) of the depletion of **1** in aqueous solution under VUV-photolysis.

The diminution of [**1**] was faster at pH 3.4 than at pH 11.0, both under air and under $N_2$. The protonation/deprotonation equilibria of **1** with the corresponding $pK_a$ values of 3.13, 4.77, 5.19 and 11 [40] are depicted in Scheme 1. At pH 3.4, the most abundant species is the monoanion of **1**, whereas at pH 11, the tri- and the tetraanions are mostly present. It might therefore be concluded that the polyanionic forms of **1** are less reactive. At both pH values, the reaction was slightly faster in the presence of $O_2$ (Figure 2 and Table 1).

**Scheme 1**. Protonation/deprotonation equilibria of citric acid (**1**).

Under acidic conditions, depletion of **1** is mainly due to the reaction with $HO^{\bullet}$ (bimolecular rate constant $k_{HO}$: $5.0 \times 10^{7}$ $M^{-1}$ $s^{-1}$ [30]). The corresponding apparent first-order kinetics (Table 1) are given by equation (9).

$$- d[\mathbf{1}]/dt = k_{HO}[HO^{\bullet}][\mathbf{1}] \quad \Rightarrow \quad [\mathbf{1}] = [\mathbf{1}]_0 \exp(-k_{app}\, t) \tag{9}$$

with $k_{HO}$: rate constant of the reaction of **1** with $HO^{\bullet}$, and $k_{app} = k_{HO}[HO^{\bullet}]$, where $[HO^{\bullet}]$ is the pseudo-stationary concentration of the short-lived $HO^{\bullet}$.

Acid **1** reacts relatively slowly with H atoms and $e^{-}_{aq}$ (rate constants of $4 \times 10^{5}$ $M^{-1}$ $s^{-1}$ and lower than $10^{5}$ $M^{-1}$ $s^{-1}$, respectively [30]). Moreover, in the presence of $O_2$, these reducing species are efficiently trapped (reactions (4) and (5)), producing $HO_2^{\bullet}$ and $O_2^{\bullet-}$ radicals that have a much lower reactivity towards organic compounds than $HO^{\bullet}$ and mainly disproportionate (reaction (7)).

Although hydroxyl radicals may react with **1** by hydrogen abstraction from the methylene groups and from the different OH groups, according to earlier findings [41], electron transfer from carboxylate anions to $HO^{\bullet}$ should be faster than hydrogen abstraction, leading in the case of the monoanion of **1** to the carboxyl radical **A** (Scheme 2). The latter may easily decarboxylate yielding the ketyl radical **B**. In the presence of $O_2$, 3-oxoglutaric acid (**3**) is readily produced from radical **B**, through $O_2$ trapping to form the peroxyl radical **C** followed by $HO_2^{\bullet}$ elimination (Scheme 2). In fact, **3** was the main intermediate product of the oxidative degradation identified by HPLC analysis. The practically exclusive formation of **3** found in this work is difficult to explain by another pathway than through initial formation of radical **A**, and may be due to the high specificity of the reaction of **1** with $HO^{\bullet}$ (electron transfer from carboxylate group). In the recently published paper on the $TiO_2$ photocatalytic degradation of citric acid in aqueous solution in the presence of oxygen [19], a similar mechanism to the one depicted in Scheme **2** was proposed.

Since the reaction of **1** with $HO^{\bullet}$ (yielding radical **A**) does not depend on $O_2$, the rate of depletion of **1** should be the same, within experimental error, in the presence and in the absence of $O_2$. However, Figure 2 shows that this was not the case, the depletion of **1** being significantly slower in the absence of $O_2$ at both pH-values investigated. This result may be explained by the reduction of radical **A** by $H^{\bullet}$ (and $e^{-}_{aq}$) produced by the VUV-photolysis of water (reactions (1) and (2)). In the absence of $O_2$ to trap efficiently these reducing species, the reduction of **A** competes with its decarboxylation and regenerates **1** (Scheme 2), leading to an apparent slower reaction of **1** with $HO^{\bullet}$. The depletion of **1** should still follow apparent first-order kinetics (equations (10) and (11)), but with $k'_{app} < k_{app}$ (equation (9)).

$$- d[\mathbf{1}]/dt = k_{HO}[HO^\bullet][\mathbf{1}] - k_H[H^\bullet][\mathbf{A}] \qquad (10)$$

with $k_H$: rate constant of the reaction of **1** with $H^\bullet$; applying the pseudo-stationary hypothesis to radical **A** leads to $[\mathbf{A}] = k_{HO}[HO^\bullet][\mathbf{1}]/(k_H[H^\bullet] + k_A)$ with $k_A$: rate constant of decarboxylation of **A,** and then to equation (11).

$$- d[\mathbf{1}]/dt = k_{HO}[HO^\bullet][\mathbf{1}] - k'[\mathbf{1}] \quad \Rightarrow \quad [\mathbf{1}] = [\mathbf{1}]_0 \exp(-k'_{app}\, t) \qquad (11)$$

with $k' = (k_{HO}[HO^\bullet]k_H[H^\bullet])/(k_H[H^\bullet] + k_A)$ and $k'_{app} = k_{app} - k'$.

This finding may be specific for VUV-photolysis, where reducing and oxidizing species are produced simultaneously in a very small reaction volume [28]. In the absence of $O_2$, the ketyl radical **B** disproportionates to product **3** and the corresponding alcohol **4** (Scheme 2). Since the alcohol may be readily reoxidized to **B** by $HO^\bullet$, it was not detected by HPLC analysis, and only **3** was found as an intermediate product, as in the presence of $O_2$.

It is noteworthy that, in the case of the UVC-photolysis of **1** in aqueous solution [42], the ketyl radical **B** was formed as one of several radicals, as shown by EPR measurements. Generation of **B** could be explained by a photochemical decarboxylation of **1** [43].

**Scheme 2**. Main pathways proposed for the oxidative degradation of citric acid (**1**) initiated by VUV-photolysis in acidic aqueous solution.

Under alkaline conditions (pH 11), consumption of **1** was slower (Table 1 and Figure 2). At this pH, the formation of $O^{\bullet-}$ must be taken into account, hence the steady state concentration of $HO^{\bullet}$ is smaller. Moreover, $O^{\bullet-}$ is less reactive and more selective than $HO^{\bullet}$, and its reaction with the tri- and the tetraanions of **1** (mostly present at pH 11) is disfavored due to coulombic repulsion.

*3.2. Gallic acid*

Air or $N_2$ saturated aqueous solutions containing 0.5 mM of gallic acid were irradiated at 20ºC and at two different pH values (2.5 and 7.5). The protonation/deprotonation equilibria and the corresponding four $pK_a$ of **2** (4.44, 8.45, 10.05 and 11.30 [44]) are shown in Scheme 3. At pH 2.5, the main species in aqueous solution is the totally protonated form, but minor amounts of the carboxylate are also present. At pH 7.5, the carboxylate is the dominant species, together with small amounts of the dianion. Since **2** is quickly oxidized in aerated alkaline solutions [3, 24, 45], no experiments were made at higher pH.

**Scheme 3.** Protonation/deprotonation equilibria of **2**.

Profiles of ln([**2**]/[**2**])$_0$ *vs.* time of irradiation in the presence and absence of dissolved $O_2$ and at pH 2.5 and 7.5 are shown in Figure 3 . Within experimental error, the depletion of **2** followed in all cases apparent first-order kinetics and the corresponding rate constants ($k_{app}$) are listed in Table 2. The pH of the reaction systems did not change significantly during the reaction time investigated.

**Figure 3.** Depletion of **2** in aqueous solution upon VUV-photolysis. Profiles of $\ln([\mathbf{2}]/[\mathbf{2}]_0)$ *vs.* time of irradiation, for $[\mathbf{2}]_0$ = 0.5 mM in the presence or absence of $O_2$ and at pH 2.5 and 7.5.

**Table 2.** Apparent first-order rate constants ($k_{app}$) of the depletion of **2** in aqueous solution under VUV-photolysis.

The rate of diminution of [**2**] was found to be almost independent of pH (slight increase at pH 7.5 compared to 2.5). This is in agreement with the small pH effect observed on the rate constants of the reaction of $HO^{\bullet}$ with **2** determined by pulse radiolysis (*e.g.* $1.1 \times 10^{10}$ and $6.4 \times 10^{9}$ $M^{-1}$ $s^{-1}$ at pH 6.8 and 0, respectively) [3].

In contrast, the rate of consumption of **2** depended strongly on the presence of dissolved $O_2$. In fact, depletion of **2** was approximately 4 times faster in air-equilibrated than in $N_2$-saturated solutions (Figure 3 and Table 2). Moreover, under the latter conditions, no mineralization was observed during the time of irradiation, whereas in air-equilibrated solutions at both pH about 5% decrease of TOC was measured after 10 minutes of irradiation, when $[\mathbf{2}]/[\mathbf{2}]_0$ was close to 0.6 (40% consumption of **2**). In addition, in the presence of $O_2$, the reaction system exhibits a yellow color (320 to 400 nm) from approximately 4 to 10 min of irradiation time, which is probably due to the formation of quinoid intermediates. Chromatograms of samples taken from reaction systems under $N_2$ or in the presence of $O_2$ show different intermediates indicating that different reaction pathways are involved depending on the experimental conditions (data not shown). However, these intermediate products could not yet be identified due to the lack of reference compounds.

From our experimental results and similarly to the case of **1**, the following mechanism could be proposed for the oxidative degradation of **2** initiated by VUV-photolysis of the aqueous system. The electron transfer from the carboxylate group of **2** to $HO^{\bullet}$ would yield radical **D** and would be followed by decarboxylation to the trihydroxyphenyl radical **E** (Scheme 4). The experimentally measured decrease of the TOC value (about 5%) at 40% conversion of **2** (vide supra) corresponds stoichiometrically to the loss of one carbon by the decarboxylation of the substrate and would agree with the proposed reaction pathway. The addition of $O_2$ to radical **E** would then lead to quinoid intermediates (explaining the yellow color observed experimentally), then to aliphatic carboxylic acids and eventually to complete mineralization.

In this context, the large effect of $O_2$ on the depletion of **2** (Figure 3) may be explained, similarly to the case of **1** (§ 3.1), by the role of the reducing species $H^{\bullet}$ (and $e^{-}_{aq}$). In the absence of $O_2$ to trap these species, the carboxyl radical **D** would be efficiently reduced, regenerating **2**. This reduction would compete with decarboxylation and should be more efficient than in the case of **1** due to the higher stability of radical **D** compared to radical **A** (Scheme 2). In fact, the rate of consumption of **2** was four times slower in the absence of $O_2$ than in its presence. The reduction of radical **D** being faster than its decarboxylation would also explain the fact that, within limits of error, no TOC decrease could be observed under $N_2$ during the same irradiation time. In the absence of $O_2$, radical **E**, resulting from decarboylation of **D**, is formed in much lower amount, and can subsequently react by hydrogen abstraction, dimerization or disproportionation, hence leading to various intermediate products that could be observed at very low concentrations by HPLC.

**Scheme 4.** Main pathways proposed for the oxidative degradation of gallic acid (**2**) initiated by VUV-photolysis in aqueous solution.

Electrophilic addition of $HO^{\bullet}$ to the aromatic system could compete with the electron transfer reaction described above. This addition would yield cyclohexadienyl (CHD) radicals as initial transient species. A variety of reaction pathways may be formally proposed for further reactions of these species, depending on the site of initial $HO^{\bullet}$ addition and on the presence of $O_2$. Two examples are presented in Scheme 4, for the addition of $HO^{\bullet}$ to the positions 1 and 4 of the aromatic ring, leading to the formation of the cyclohexadienyl radicals **F** and **G**, respectively. In the presence of $O_2$, CHD radicals may be trapped by $O_2$ and lead to decarboxylated and/or quinoid intermediate products, and the observed decrease of TOC could be due to oxidative degradation of the aromatic ring, besides decarboxylation. Based on the assumption of formation of CHD radicals, two mechanistic hypotheses may be formulated for explaining the much lower rate of consumption of **2** under reductive experimental conditions ($N_2$-saturated solutions): i) the reversibility of the addition of $HO^•$ to **2**; ii) the formation of phenoxyl radicals that could be reduced back to **2** by recombination with H atoms (or $e^-_{aq}$) (Scheme 4). In the absence of $O_2$, addition of $HO^•$ to position 1 or 2 cannot lead to such phenoxyl radicals. However, CHD radicals formed by addition of $HO^•$ to position 3 or 4 may be dehydrated to phenoxyl radical intermediates that, in the absence of $O_2$, could recombine with $H^•$ giving **2** (as shown in Scheme 4 for addition to position 4). In this case, the phenoxyl radicals are not the initial intermediates formed by the reaction of **2** with $HO^•$, and apparent first-order kinetics for the disappearance of **2** is not expected. The latter type of kinetics was actually observed experimentally (Figure 3). However the conversion rate under $N_2$ is lower than 15% and the contribution of an oxidation/reduction cycle involving phenoxyl radicals cannot be totally discarded. It should be noted that the formation of phenoxyl radicals has been observed by pulse radiolysis in the absence of $O_2$ [3]. The authors propose that phenoxyl radicals could result from the reaction of a primary transient adduct (of unspecified nature) with a second molecule of **2** at neutral pH, or from the acid and base catalysed dehydration of initially formed CHD in acidic and alkaline solutions.

## 4. Conclusions

VUV-photolyses of aqueous solutions of citric acid (**1**) and gallic acid (**2**) led to the oxidation of both substrates. The rate of depletion of **1** was found to be dependent on the pH of the reaction system. At acidic pH (3.4), depletion was faster than under alkaline conditions (pH 11). This effect may be explained by the smaller steady-state concentration of $HO^{\bullet}$ radicals at pH 11 due to their deprotonation and by a diminished reactivity of $O^{\bullet-}$ because of coulombic repulsion. In the case of **2**, the variation of pH in the range investigated (2.5 to 7.5) did not affect the rate of the reaction, in agreement with the small effect of the pH on the rate constant of the reaction of $HO^{\bullet}$ with **2**. The depletion of both substrates was slower in the absence of $O_2$, and the effect was much more pronounced for **2** than for **1**. These results may be explained assuming that the oxidative degradation of **1** and **2** is initiated in both cases by an electron transfer reaction to $HO^{\bullet}$, yielding the intermediate carboxyl radicals **A** (Scheme 2) or **D** (scheme 4), respectively. The lower rates observed in the absence of $O_2$ would then be due to an efficient reduction of radicals **A** or **D** by $H^{\bullet}$ (and $e^-_{aq}$) produced together with $HO^{\bullet}$ during the VUV-photolysis of water. This reduction competes with the radical decarboxylation, and regenerates the substrate, leading to an apparent slower reaction rate with $HO^{\bullet}$. The higher stability of the intermediate radical **D** compared to **A** could be responsible for the larger effect of $O_2$ observed in the case of **2**. However, at this stage of the investigation, a contribution of the electrophilic addition of $HO^{\bullet}$ to the aromatic system of **2** generating phenoxyl radicals cannot be discarded.

**Acknowledgements**

The authors acknowledge the financial support by Hewlett-Packard Deutschland GmbH. This work was performed as part of Agencia Nacional de Promoción Científica y Tecnológica (ANPCyT) project PICT2003-13-13261. N.Q. thanks CNEA-CONICET for a doctoral fellowship, DAAD for a student fellowship and Profs. A.M.B. and E.O. for the extension of her stay in Karslruhe. M.I.L. is a member of CONICET.

**References**

[1] F.J. Beltrán, J.M. Encinar, J.F. García-Araya, Wat. Res. 27 (1993) 1023-1032.

[2] Y.-X. Sheng, L. Li, Q. Wang, H.-Z. Guo, D.-A. Guo, J. Pharm. Biom. Anal. 37 (2005) 805-810.

[3] P. Dwibedy, G.R. Dey, D.B. Naik, K. Kishore, P.N. Moorthy, Phys. Chem. Chem. Phys. 1 (1999), 1915-1918.

[4] F.J. Benítez, F.J. Real, J.L. Acero, A.I. Leal, C. Garcia, J. Hazard. Mater. B126 (2005) 31-39.

[5] E. Danačiková-Popelová, J. John, K. Rosiková, F. Sebesta, E.W. Hooper, Fourth International Symposium and Exhibition on Environmental Contamination in Central and Eastern Europe, Warsaw98 Proceedings, Sept. 15-17, 1998, 569-575. Publ.: Institute for International Cooperative Environmental Research, Florida State University, Tallahassee, Fla.

[6] S.J. Keny, A.G. Kumbhar, G. Venkateswaran, K. Kishore, Rad. Phys. Chem. 72 (2005) 475-482.

[7] O. Legrini, E. Oliveros, A.M. Braun, Chem. Rev. 93 (1993) 671-698.

[8] M.I. Litter. Introduction to photochemical advanced oxidation processes for water treatment. In The Handbook of Environmental Chemistry. Vol. 2, Part M (2005), Environmental Photochemistry Part II. Boule P.; Bahnemann D.W.; Robertson P.K.J. Eds. Springer-Verlag, Berlin Heidelberg 2005, pp. 325-366. Vol. 2, Part M (2005), Environmental Photochemistry Part II.

[9] M.R. Hoffman, S.T. Martin, W. Choi, D.W. Bahnemann, Chem. Rev. 95 (1995) 69-96.

[10] X. Doménech, W. Jardim, M. Litter. “Tecnologías avanzadas de oxidación para la eliminación de contaminantes”, X. Domènech, W. Jardim y M. Litter, in: Eliminación de contaminantes por fotocatálisis heterogénea. Texto colectivo elaborado por la Red CYTED VIII-G, M.A. Blesa y B. Sánchez Cabrero (Eds.), Ediciones CIEMAT, Madrid, España, 2004, pp. 7-34.

[11] M.I. Litter, Appl. Catal. B: Environ., 23 (1999) 89-114.

[12] I. Mazzarino, P. Piccinini, Chem. Eng. Sci. 54 (1999) 3107-3111.

[13] M.R. Prairie, L.R. Evans, S.L. Martínez, Chem. Oxid. 2 (1992) 428-441.

[14] M.R. Prairie, B.M. Stange, L.R. Evans, in: Photocatalytic Purification and Treatment of Water and Air, 353-63 (1993).

[15] M.R. Prairie, L.R. Evans, R. Lindsey, B.M. Stange, S.L. Martinez, Environ. Sci. Technol. 27 (1993) 1776-1782.

[16] G. Colón, M.C. Hidalgo, J.A. Navío, Langmuir 17 (2001) 7174-7177.

[17] C.J. Dodge, A.J. Francis, Environ. Sci. Technol. 28 (1994) 1300-1306.

[18] C.J. Dodge, A.J. Francis, Environ. Sci. Technol. 36 (2002) 2094-2100.

[19] N. Quici, M.E. Morgada, R.T. Gettar, M. Bolte, M.I. Litter, Appl. Catal. B: Environ., 71 (2006) 117-124.

[20] W. Gernjak, T. Krutzler, A. Glaser, S. Malato, J. Cáceres, R. Bauer, A.R. Fernández-Alba, Chemosphere 50 (2003) 71-78.

[21] G. Lofrano, S. Meriç, V. Belgiorno, R.M.A. Napoli, Desalination 211 (2007) 10-21.

[22] K. Nam, W. Rodríguez, J.J. Kukor, Chemosphere 45 (2001) 11-20.

[23] M.A. Miranda, F. Galindo, A.M. Amat, A. Arques, Appl. Cat. B: Environ. 30 (2001) 437-444.

[24] M. Carbajo, F.J. Beltrán, F. Medina, O. Gimeno, F.J. Rivas, Appl. Catal. B: Environ. 67 (2006) 177-186.

[25] I. Gassiot, C. Baus, K. Schaber, A.M. Braun, J. Inf. Rec. 24, 129-132 (1998) VUV Gas-Phase Photooxidation: A New Tool for the Degradation of VOCs in Air.

[26] US/EPA Handbook of Advanced Photochemical Oxidation Processes (1998). EPA/625/R-98/004.

[27] T. Oppenländer, "Photochemical Purification of Water and Air", Wiley-VCH, Weinheim, Germany, 2002.

[28] M.G. González, E. Oliveros, M. Wörner, A. M. Braun, J. Photochem. Photobiol., C: Reviews, 5 (2004) 225-246.

[29] G. Heit, A. Neuner, P.-Y. Saugy, A.M. Braun, J. Phys. Chem. 102 (1998) 5551-5561.

30] G.V. Buxton, C.L. Greenstock, W.P. Helman, A.B. Ross, J. Phys. Chem. Ref. Data, 17 (1988) 513-886.

[31] R.A. Holroyd, H.J. Bielski, J. Am. Chem. Soc. 100 (1978) 5796-5800.

[32] K. Azrague, E. Bonnefille, V. Pradines, V. Pimienta, E. Oliveros, M.T. Maurette, F. Benoit-Marquié, Photochem. Photobiol. Sci. 4 (2005) 406-408.

[33] B.H.J. Bielski, D.E. Cabelli, Int. J. Radiat. Biol. 59 (1991) 291-319.

[34] M.C. Gonzalez, G. Carrillo Le Roux, J.A. Rosso, A.M. Braun, Chemosphere, in press.

[35] M.C. Gonzalez, A.M. Braun, A. Bianco Prevot, E. Pelizzetti, Chemosphere 28 (1994) 2121-2127.

[36] M.C. González, A.M. Braun. Res. Chem. Intermed. 21 (1995) 837-859.

[37] Zs. László, A. Dombi, Chemosphere 46 (2002) 491-494.

[38] M.C. Gonzalez, A.M. Braun, J. Photochem. Photobiol. A: Chem. 93 (1996) 7-19.

[39] M.C. González, A.M. Braun, J. Photochem. Photobiol. A: Chem. 95 (1996) 67-72.

[40] A.E. Martell and R.M. Smith, Critical Stability Constants. Vol. 5 (Plenum Press, New York and London, 1974), pp. 329.

[41] I.G. Draganić and Z.D. Draganić, The radiation chemistry of water (Academic Press, New York and London, 1971), p. 101.

[42] H. Zeldes, R. Livingston, J. Am. Chem. Soc. 93 (1971) 1082-1085.

[43] D. J. Coyle, Chem. Rev. 78 (1978) 97-123.

[44] M. Fukushima, S. Tanaka, K. Hasebe, M. Taga, H. Nakamura, Anal. Chim. Acta 302 (1995) 365-373.

[45] K. Polewski, S. Kniat, D. Sławińska, Curr. Topics Biophys. 26 (2002) 217- 227.

**Legends of Tables, Figures and Schemes**

**Table 1**. Apparent first-order rate constants ($k_{app}$) of the depletion of **1** in aqueous solution under VUV photolysis.

**Table 2.** Apparent first-order rate constants ($k_{app}$) of the depletion of **2** in aqueous solution under VUV photolysis.

**Figure 1.** Consumption of citric acid (**1**) in air-equilibrated aqueous solution upon VUV photolysis. Profiles of [**1**]/[**1**]$_0$ *vs.* time of irradiation at different initial concentrations of **1** ([**1**]$_0$); pH 3.4, 20°C.

**Figure 2.** Depletion of citric acid (**1**) in aqueous solution upon VUV photolysis. Profiles of ln([**1**]/[**1**]$_0$) *vs.* time of irradiation, for [**1**]$_0$ = 0.5 mM in the presence or absence of $O_2$ and at pH 3.4 and 11.0 (20ºC).

**Figure 3.** Depletion of gallic acid (**2**) in aqueous solution upon VUV photolysis. Profiles of ln([**2**]/[**2**]$_0$) *vs.* time of irradiation, for [**2**]$_0$ = 0.5 mM in the presence or absence of $O_2$ and at pH 2.5 and 7.5 (20ºC).

**Scheme 1.** Protonation/deprotonation equilibria of citric acid (**1**).

**Scheme 2.** Main pathways proposed for the oxidative degradation of citric acid (**1**) initiated by VUV photolysis in acidic aqueous solution.

**Scheme 3.** Protonation/deprotonation equilibria of **2**.

**Scheme 4.** Main pathways proposed for the oxidative degradation of gallic acid (**2**) initiated by VUV photolysis in aqueous solution.

**Table 1** Apparent first-order rate constants ($k_{app}$) of the depletion of **1** in aqueous solution under VUV-photolysis.

| Conditions | $k_{app}$ ($s^{-1}$) × $10^4$ |
|---|---|
| | Citric acid (**1**) |
| pH 3.4 – air | 5.45 |
| pH 3.4 – $N_2$ | 4.55 |
| pH 11.0 – air | 4.32 |
| pH 11.0 – $N_2$ | 3.25 |

**Table 2.** Apparent first-order rate constants ($k_{app}$) of the depletion of **2** in aqueous solution under VUV photolysis.

| Conditions | $k_{app}$ ($s^{-1}$) × $10^4$ |
|---|---|
| | Gallic acid (**2**) |
| pH 2.5 – air | 8.98 |
| pH 2.5 – $N_2$ | 2.02 |
| pH 7.5 – air | 8.75 |
| pH 7.5 – $N_2$ | 2.88 |

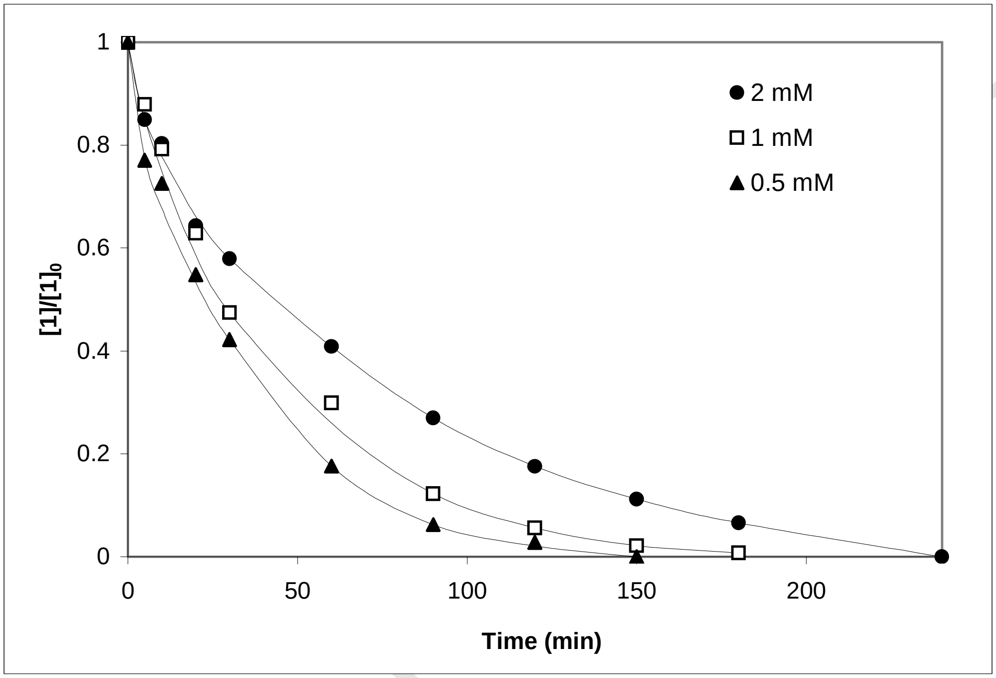


**Figure 1**

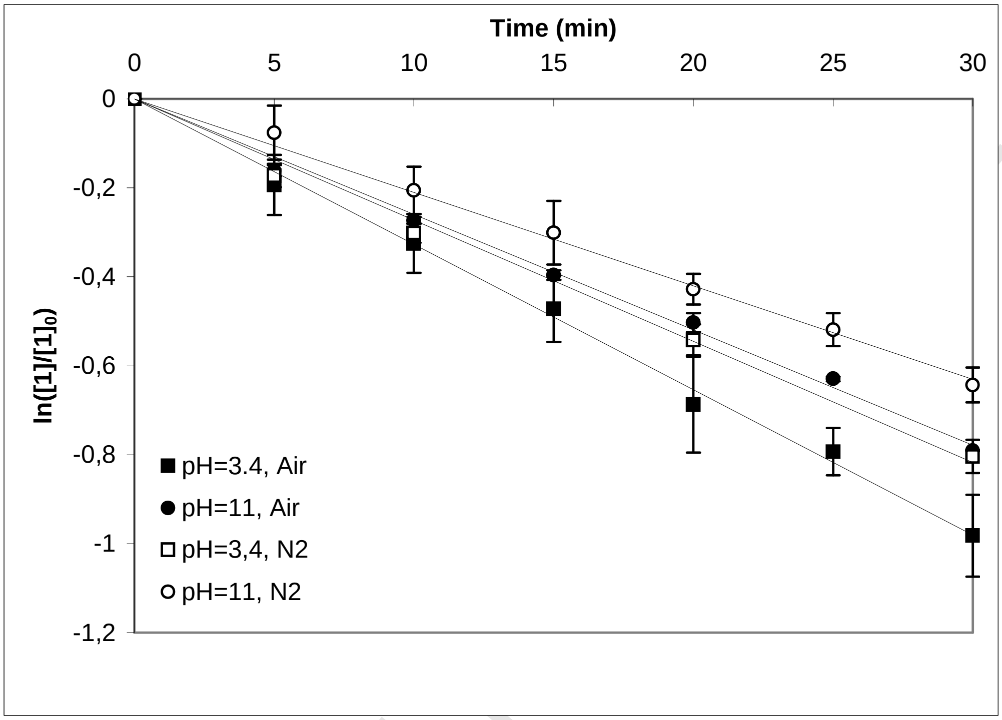
Time (min)
0
5
10
15
20
25
30
0
-0,2
-0,4
-0,6
-0,8
-1
-1,2
ln([1]/[1]0)
pH=3.4, Air
pH=11, Air
pH=3,4, N2
pH=11, N2

**Figure 2**

**Figure 3**

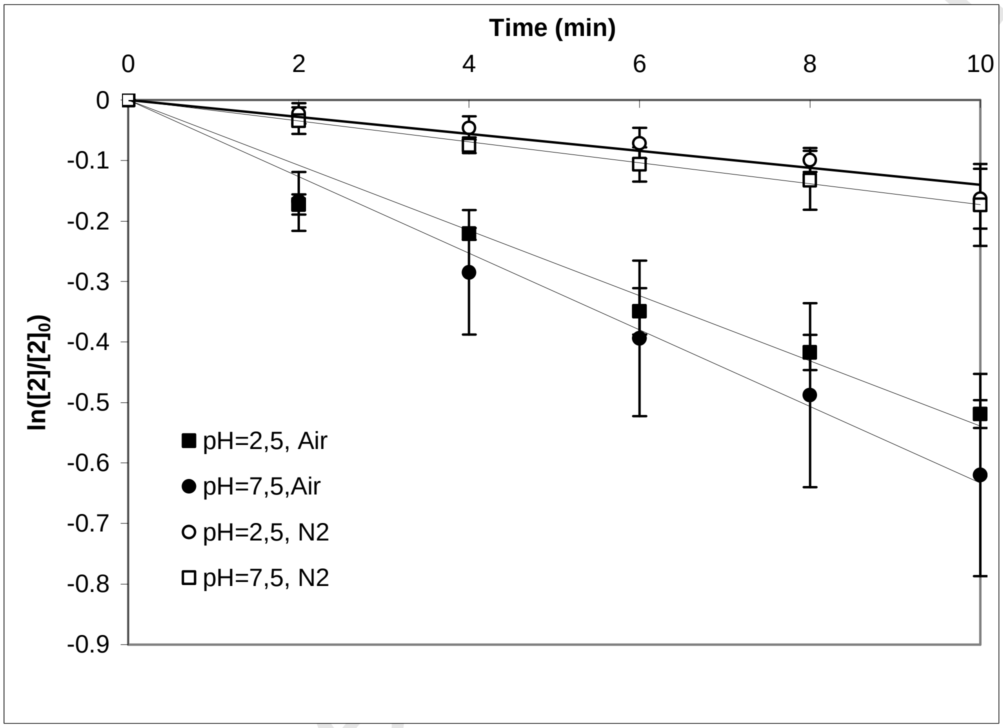
Time (min)
0
2
4
6
8
10
0
-0.1
-0.2
-0.3
-0.4
-0.5
-0.6
-0.7
-0.8
-0.9
ln([2]/[2]$_0$)
pH=2,5, Air
pH=7,5,Air
pH=2,5, N2
pH=7,5, N2

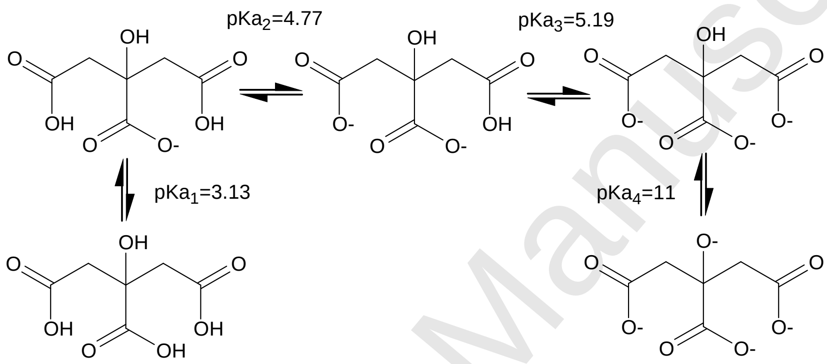


**Scheme 1**

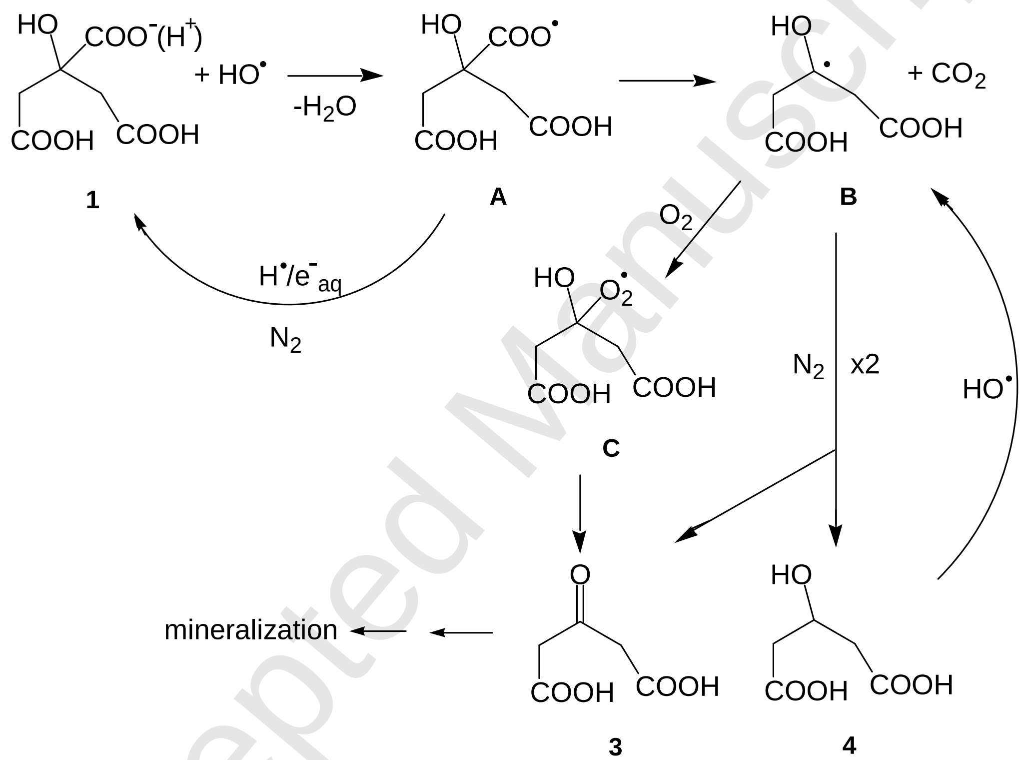

HO
COO-(H+)
+ HO•
-H2O
COOH
COOH
1
HO
COO•
COOH
COOH
A
HO
+ CO2
COOH
COOH
B
O2
H•/e-aq
N2
HO
O2•
COOH
COOH
C
N2
x2
HO•
O
COOH
COOH
3
mineralization
HO
COOH
COOH
4


**Scheme 2**

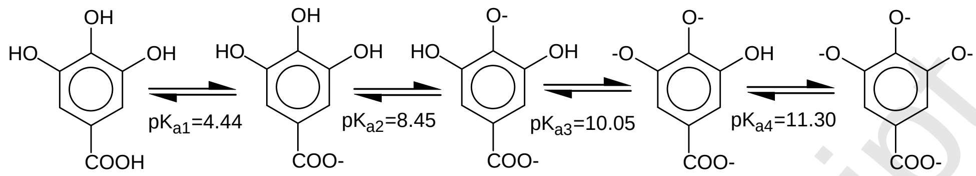


**Scheme 3**

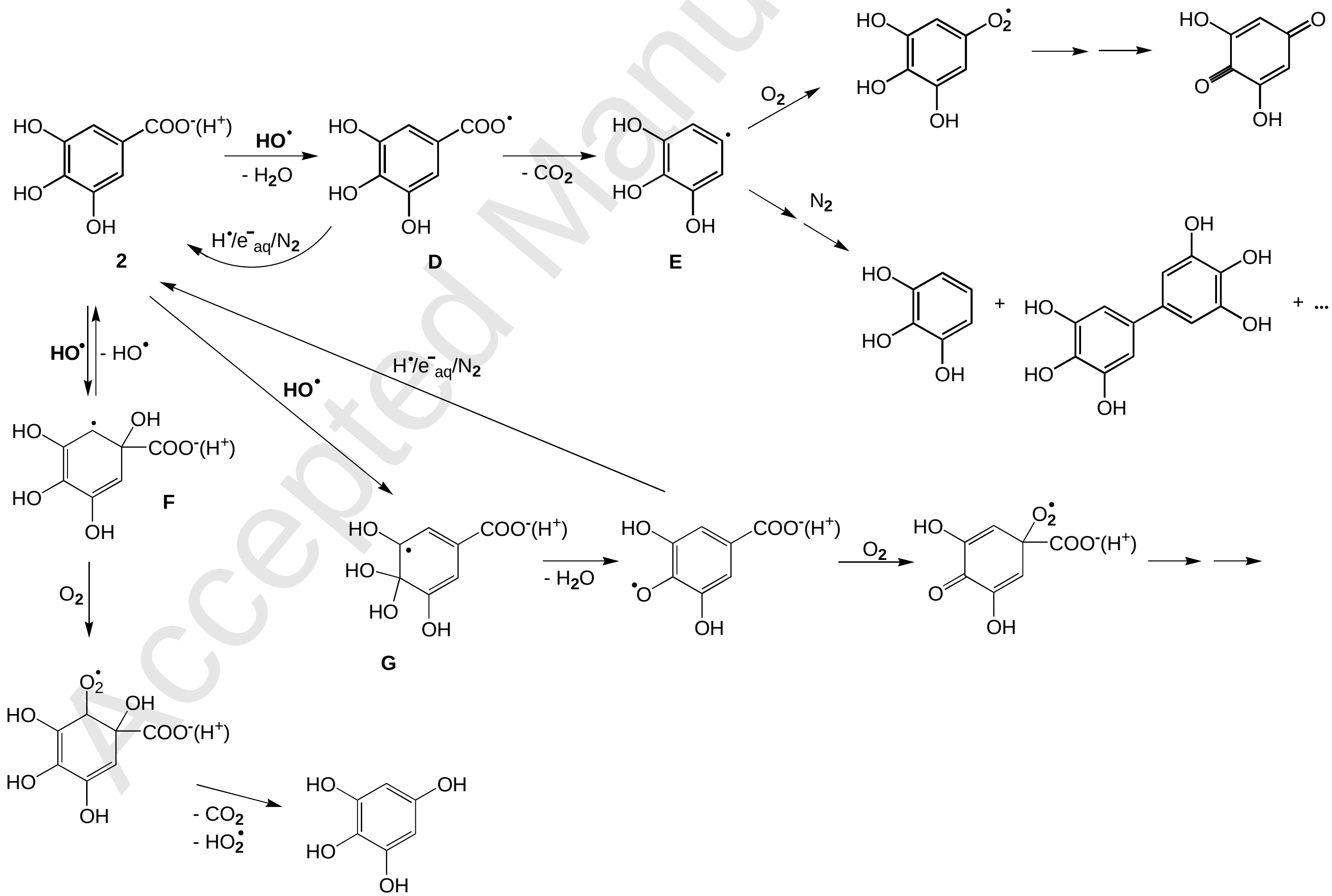


**Scheme 4**